IEEE Access
Multidisciplinary | Rapid Review | Open Access Journal

Date of publication xxxx 00, 0000, date of current version xxxx 00, 0000.

*Digital Object Identifier 10.1109/ACCESS.2017.Doi Number*

# Multi-Rotor Virtual Machine for Grid-forming Converter to Damp Sub-synchronous Resonances

**Ngoc Bao Lai[1,2], Student, IEEE, Gregory N. Baltas[1,3], Student, IEEE, and Pedro Rodriguez[1,2], Fellow, IEEE**

[1]Environmental Research and Innovation department, Luxemburg Institute of Science and Technology, L-4362 Esch-sur-Alzette, Luxembourg.
[2]Universitat Politècnica de Catalunya (UPC), 08034 Barcelona, Spain.
[3]Universidad Loyola, 41704 Sevilla, Spain.

Corresponding author: Ngoc Bao Lai (e-mail: ngocbao.lai@list.lu).

This work was supported in part by the European Commission under Project FLEXITRANSTORE-H2020-LCE-2016-2017-SGS-774407, and in part by the Spanish Ministry of Science under Project ENE2017-88889-C2-1-R.

**ABSTRACT** Grid-forming power converters (GFMC) have been widely adopted in power systems as an attractive solution against the challenges imposed by the ever-increasing penetration of renewables. Despite its versatility, GFMC is employed only to provide islanded operation, grid regulations, and synthetic inertia. To further extend the use of GFMC in enhancing power system stability, this paper proposes a multi-rotor virtual machine (MRVM) controller to attenuate sub-synchronous oscillations. Driven by the formulation of a virtual synchronous machine (VSM), the proposed MRVM implements a VSM-based GFMC with several virtual rotors whose electromechanical characteristics can be individually adjusted to target specific oscillatory modes in the system. In this work, the MRVM's working principle is described in detail and tuning guidelines are proposed to simplify the selection of control parameters by using frequency-domain techniques and the eigenvalue locus analyses. To validate the performance of the MRVM, an IEEE benchmark grid model is adopted namely, the three-machine-infinite-bus system. It is evident from the results that the MRVM (i) provides higher degrees of freedom when dealing with sub-synchronous oscillations, and (ii) outperforms conventional GFMC, especially in damping intra-area power oscillations.

**INDEX TERMS** Frequency-selective damping, grid-forming power converter, power oscillation damping, sub-synchronous oscillation, virtual synchronous machine.

## I. INTRODUCTION

Low-frequency oscillations (LFO) exist naturally in power systems due to the power exchange between generating units operating in parallel and when interconnected through long transmission lines [1], [2]. Such phenomenon was expected and studied since the early development stages of electricity networks. However, the energy transition towards clean energy systems has aroused a renewed interest in the electromechanical interactions within the frequency range of 0.1 to 2.0 Hz [3]. In fact, the wide integration of power electronics is not only affecting the characteristics of the existing modes of oscillations but also creates new ones [4], which affects the power system performance, since operators must enforce conservative limits on the maximum allowable power transfer in transmission lines to ensure the stability of the system. Such restrictions, however, introduce substantial costs reducing social welfare [5]. Therefore, damping of low-frequency electromechanical oscillations is imperative both in terms of stability and efficiency.

The necessity of mitigating undamped power oscillations has been widely recognized by the industry and academia since the 1960s [6], [7]. In addition, numerous incidents related to sub-synchronous resonances (SSR) have been reported around the world. For instance, the SSR events at Mohave power plant in Nevada, USA in 1970 and in 1971 [8]; at the Shangdu power plant in the inner, Mongolia, China in 2011 [9]; and at power plants of the Electric Reliability Council of Texas (ERCOT) area in 2012 [10], to name a few.

Power System Stabilizer (PSS) have been the most cost-efficient method for providing additional damping to LFO, usually through the excitation system of the generator [11]. In the literature, there are different types of PSS and tuning

This article has been accepted for publication in a future issue of this journal, but has not been fully edited. Content may change prior to final publication. Citation information: DOI 10.1109/ACCESS.2021.3112070, IEEE Access



procedures [12] although in many cases the PSS parameters are set upon plant commissioning and updated only sporadically [13]. However, placement of the PSS as well as its tuning are critical for achieving optimal results. With power electronics displacing many of the existing fossil-fueled power plants [14]: (i) suitable PSS installation sites will become fewer and (ii) the number of already installed PSS will decrease (and so will the damping of critical modes).

As a viable alternative to PSS, some LFO dampers based on the flexible alternating current transmission system (FACTS) have been proposed in the literature. For instance, the sliding mode controller and the robust linear quadratic regulator have been employed in a static synchronous compensator (STATCOM) [15] and in a thyristor controlled series compensator (TCSC) [16] to damp electromechanical modes. Other damping strategies for FACTS devices are reported in [17] and [18]. As the installation of renewables and energy storage systems (ESS) has increased in recent years, the use of power converters for suppressing mechanical interactions within power systems has become even more practical. Notably, optimization approaches and proportional-integral-derivative controller were proposed to leverage ESS [19] and photovoltaic systems [20] to reduce SSR.

Nevertheless, the above approaches only focus on maximizing the LFO damping of the power converter, which is not always practical. That is, in addition to LFO damping, power converters are often required to provide multiple functionalities and services to withstand and support the grid under abnormal operating conditions, such as in the case of voltage sags, and under low-inertia situations [21], [22]. Consequently, it is not straightforward to design and tune separately the individual controller for each of the said functionalities such that the closed-loop system can work in a stable and reliable manner.

To overcome such a challenge, the grid-forming converter (GFMC) concept has been proposed. GFMC refers to a group of strategies that control grid-connected converters as a controlled voltage source [23], [24]". According to ENTSO-E, a GFMC should be able to support the operation of the ac power system under normal, alerted, emergency, blackout and restoration states without having to rely on services from synchronous generators [25]. In fact, the GFMC implementation, especially those based on virtual synchronous machine (VSM) e.g. the synchronous power controller (SPC), allows unifying multiple control functions in a single cascaded control structure [26]. It has been demonstrated in this regard that, among other functionalities, the SPC can provide current control, voltage control, power control, inertia emulation, droop control, and power oscillation damping [26].

Similar to a synchronous machine (SM), the SPC could provide LFO damping through the virtual admittance and the virtual inertia. In order to adjust the damping power

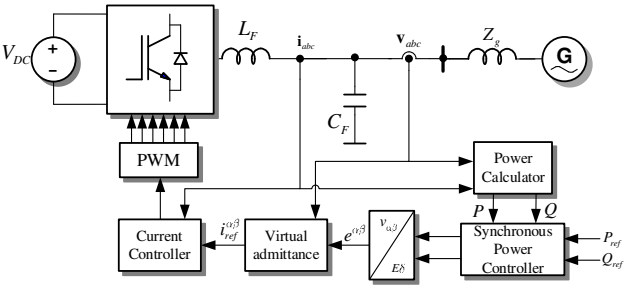


**Fig. 1. SPC-based GFMC connected to an infinite bus.**

provided by the SPC, an analytical method is proposed in [27]. According to [27], the participation of the SPC towards the damping of electromechanical oscillations can be increased by properly tuning the virtual inertia and damping coefficient. However, as the damping coefficient also determines the dynamic behavior of the SPC, reducing the damping ratio as suggested in [27] certainly deteriorates the overall performance of the GFMC. To overcome such a limitation, selective damping methods have also been reported [28] and [29]. However, there have been any studies that deal with the implementation of multi-band LFO damper for GFMC in a systematic manner.

This paper brings a new concept, i.e. multi-rotor virtual machine (MRVM), for improving oscillation damping performance of GFMC while retaining its overall dynamic characteristics. Indeed, the MRVM exploits the flexibility of power converters to implement a VSM with multiple rotors to realize a GFMC with a high degree of freedom in coping with LFO. That is, by emulating multiple rotors (instead of only one) within the framework of a VSM, the MRVM can be tuned to attenuate selectively oscillatory modes. Frequency-domain techniques and modal analyses are employed to identify the optimal settings for the MRVM. The proposed control approach is validated with the three-machine infinite bus (3MIB) IEEE benchmark system. Validation results confirm that the proposed MRVM can simultaneously improve the damping of both local and inter-area modes.

The rest of the paper is organized as follows. Section II reviews the use of GFMC for damping LFO and highlights the limitations of the existing approaches. Section III describes the concept and parameter tuning of the proposed MRVM. Section IV presents simulation validation of the MRVM using the 3MIB system. Finally, section V summarizes the main outcomes and contributions of the paper.

## II. DAMPING LFO WITH GRID-FORMING CONVERTERS

To assess the performance of GFMC in damping SSR, the SPC-based GFMC (SPC-GFMC) is considered. In general, the SPC-GFMC consists of three control loops dedicated to providing three sets of grid functionalities, shown in Fig. 1. The current control loop ensures that the injected currents follow their references with minimal settling times. According to grid codes [30], the current controller is also required to

This article has been accepted for publication in a future issue of this journal, but has not been fully edited. Content may change prior to final publication. Citation information: DOI 10.1109/ACCESS.2021.3112070, IEEE Access



minimize the harmonic components in the injected currents. Likewise, the voltage control loop, implementing the virtual admittance, is often parameterized according to the voltage support requirements [31]. The virtual admittance block can be understood as the stator part of an SM. The outermost loop, i.e. the power controller often implements a swing equation to mimic the electromechanical behavior of an SM for providing grid synchronization, inertia emulation, and/or power oscillation damping to name a few.

As these three control loops are nearly decoupled from one another, it is convenient to discard the dynamics of the current and voltage control loops when investigating the electromechanical characteristic of the SPC-GFMC [32]. This simplification is reasonable, since SSR are often in the range of 0.1 to 2Hz [33], while current and voltage perturbations show much higher frequencies. According to [32], the small-signal model of the SPC-GFMC might be given as in Fig. 2, where $H$ and $D$ are virtual inertia constant and virtual damping coefficient, respectively, $\omega_g^0$ is the nominal grid frequency, $\Delta\delta$ denotes virtual rotor angle, $\Delta P_e$ is the deviation of the error in active power, and $Y_v$ is the virtual admittance. As the dynamics of the virtual admittance block is much faster than those of the power control loop, only RMS value of the admittance is considered in this paper. Note that the closed-loop control scheme of the SPC-GFMC has 2 inputs, the active power reference $\Delta P_{ref}$ and the grid frequency $\Delta\omega_g$. The output is the injected active power $\Delta P$.

Thus, it is possible to derive the closed-loop transfer functions from the inputs to the output as follow:

$$G_{P2P}(s) = \frac{Y_v\omega_g^0}{2Hs^2 + Ds + Y_v\omega_g^0} \tag{1}$$

$$G_{\omega 2P}(s) = \frac{2HY_v\omega_g^0 s + DY_v\omega_g^0}{2Hs^2 + Ds + Y_v\omega_g^0}. \tag{2}$$

As (1) and (2) take the form of a second-order system which is often given by the following transfer function.

$$G(s) = \frac{\omega_n^2}{s^2 + 2\zeta\omega_n s + \omega_n^2} \tag{3}$$

where $\zeta$ and $\omega_n$ are the damping ratio and natural frequency.

In practice, damping is often given in terms of damping ratio $\zeta$ rather than damping coefficient $D$. Therefore, the damping coefficient $D$ is calculated from the damping ratio $\zeta$ using (3) as:

$$D = \sqrt{8HY_v\zeta^2\omega_g^0}. \tag{4}$$

From (1) and (2), the step response and frequency characteristic can be obtained as in Fig. 4 and Fig. 3, respectively. In normal operating conditions, to achieve a proper dynamic response for the SPC-GFMC, the damping

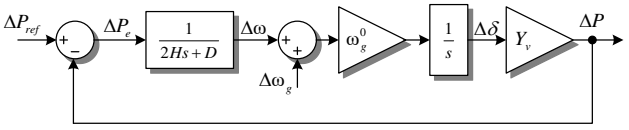


**Fig. 2. Small-signal model of SPC-GFMC.**

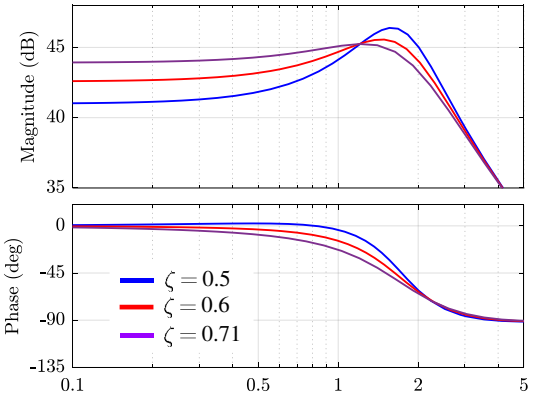


**Fig. 3. Frequency response of SPC-GFMC according to (2).**

ratio $\zeta$ is often set to 0.71. As shown in Fig. 4, with $\zeta = 0.71$, the step response of the active power is rather stable with negligible overshoot. In addition, Fig. 3 shows that the SPC-GFMC has high gain at low frequency i.e. less than 1 Hz. meaning that it can provide damping to SSR. Such damping, however, might not be significant to LFO whose frequency is above 1 Hz because of the substantial phase lag at higher frequencies. In fact, the phase delay is approximately 45 degrees at 1.5 Hz.

To improve the performance of the SPC-GFMC, a tuning method is proposed in [27]. Essentially, this tuning approach aims to reduce the phase lag by adjusting the controller damping ratio $\zeta$. As shown in Fig. 3, when the damping ratio decreases, the phase lag decreases, resulting in better damping at a higher frequency, i.e. higher than 1 Hz. This method might be of interest in certain applications where power oscillation damping is the primary objective. Nevertheless, it is obvious from Fig. 4 that reducing the damping ratio harms the overall dynamic performance of the SPC-GFMC. Indeed, the lower the damping ratio the higher the overshoot of the step response. In other words, this method increases the damping capabilities by reducing the overall system stability. This is not desirable as system stability needs to be ensured at all times. Moreover, decreasing the damping ratio also reduces the gain at lower frequencies, causing the degradation of damping performance against interarea modes. Hence, this method is not suitable for dealing with multiple modes simultaneously.

On the other hand, the work in [34] demonstrated that frequency-selective damping methods might offer better performance in suppressing LFO. Motivated by such a demonstration, this paper coins a new concept, namely MRVM, to fully exploit the virtualization paradigm in controlling GFMC. That is, instead of emulating a conventional VSM, MRVM will implement a virtual

This article has been accepted for publication in a future issue of this journal, but has not been fully edited. Content may change prior to final publication. Citation information: DOI 10.1109/ACCESS.2021.3112070, IEEE Access



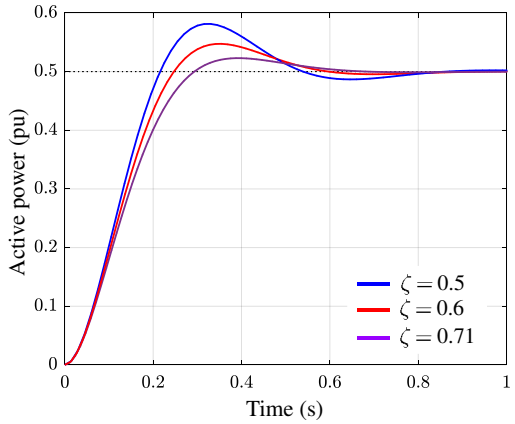


**Fig. 4. Active power of the SPC-GFMC when power reference undergoes a step change of 0.5 pu.**

machine that consists of multiple virtual rotors to attenuate simultaneously several modes in the power system with a high degree of controllability.

Assuming that frequencies of the oscillatory modes are well-detected by using the techniques presents in [28] and [29], this paper will be focused on analyzing the operation and design of the MRVM, and not the detection of the oscillations' frequency.

## III. MULTI-ROTOR VIRTUAL MACHINE CONTROLLER

### A. CONTROL STRUCTURE

The conceptual representation of the proposed MRVM is shown in Fig. 5. The main idea of the MRVM is to leverage the flexibility of the digital implementation of the control system for a GFMC to implement enhanced functionalities. Overall, MRVM consists of two main control blocks, namely, the decoupling network and the virtual rotors. The decoupling network is used to set the target oscillation frequencies while the virtual rotors dictate the desired damping toward such frequencies. Unlike conventional VSM implementation, the MRVM emulates a VSM with several virtual rotors. Each of the virtual rotors will have different mechanical characteristics for creating selective responses to different oscillatory modes.

Indeed, the main rotor, rotating at $\omega_0$, can be tuned by adjusting $\{H_0, D_0\}$ to provide the overall electromechanical behavior of the GFMC. Whereas the other virtual rotors, rotating at $\omega_1$ and $\omega_2$, can be tuned with $\{H_1, D_1\}$ and $\{H_2, D_2\}$, respectively, to provide adjustable damping to different electromechanical modes. In this way, the damping of GFMC to LFO can be maximized in a selective manner without comprising significantly the overall performance of the GFMC.

The detailed implementation of the proposed MRVM is shown in Fig. 6. While the electromagnetic part, i.e. the virtual admittance is adopted from the SPC-GFMC, the structure of the electromechanical part is substantially modified to deal with multiple LFO in the power system. Apart from the additional virtual rotors to target specific modes, a decoupling

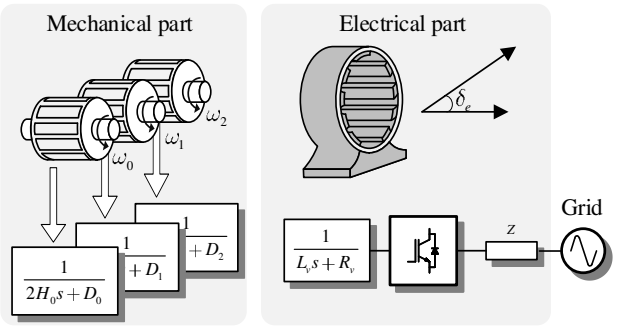


**Fig. 5. Conceptual presentation of the proposed MRVM.**

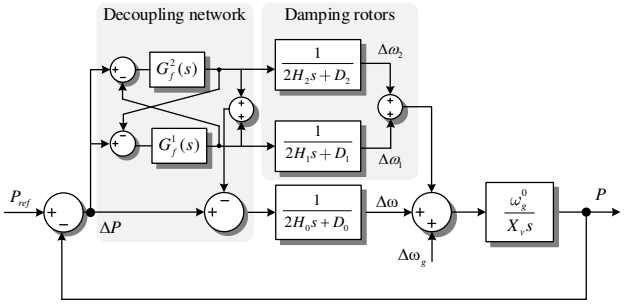


**Fig. 6. Detailed block diagram of the proposed MRVM.**

network is introduced. Such a decoupling network consists of band-pass filters and crossed cancellation of filtered signals which is important to improve the filtering performance. The decoupling network is particularly essential to separate the dynamics between virtual rotors. Thus making selective attenuation of the oscillatory modes possible. Furthermore, decoupling the dynamics of the virtual rotors also simplifies greatly the tuning of the control parameters.

### B. PARAMETER TUNING

Commonly, there are multiple oscillatory modes in power systems. Electromechanical modes, characterized by generators' inertia, line impedances, governors, and AVRs, are often of frequency from 0.1 to 2 Hz. Based on the nature of the interactions between the generators or the group of generators, these modes are classified into intra-area (local) and interarea modes. The frequency of interarea modes ranges from 0.1 to 0.8 Hz, whereas the power oscillations between generators in the same area are normally of higher frequency e.g. from 0.7 to 2 Hz [35].

Without loss of generality and for demonstrating the working principle of MRVM, two electromechanical modes, local (1.25 Hz) and interarea (0.4 Hz), are considered in the following analyses. As stated previously, these frequencies can be provided by a prediction algorithm, therefore here are assumed to be known. It is clear from Fig. 7 that the conventional SPC-GFMC can provide effective damping to interarea mode owning to high gain and low phase lag. However, local modes are almost out of the scope of SPC-GFMC due to the high phase lag i.e. approximately 40 degrees.

This article has been accepted for publication in a future issue of this journal, but has not been fully edited. Content may change prior to final publication. Citation information: DOI 10.1109/ACCESS.2021.3112070, IEEE Access



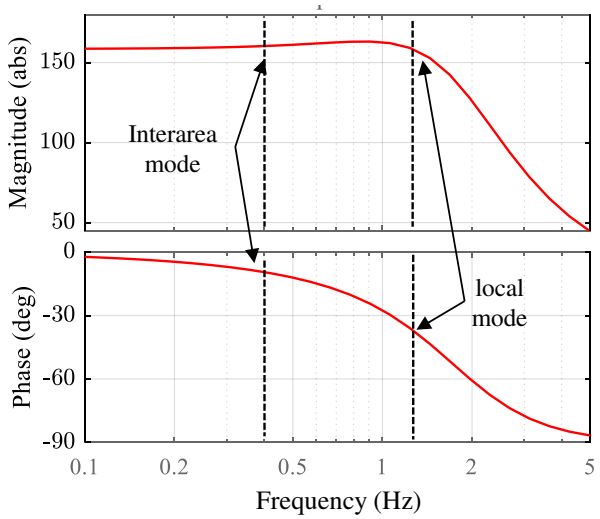


**Fig. 7. Frequency response of an SPC-GFMC and target LFO modes.**

For convenience, the electromagnetic part of the MRVM can be rewritten as

$$G_{ma}(s)=\frac{\omega_g^0}{X_v s} \tag{5}$$

with $X_v$ being the virtual impedance.

Likewise, the virtual rotors emulating swing equations can be formulated as

$$G_{sw,i}=\frac{1}{2H_i s+D_i} \tag{6}$$

where subscript $i=0$, $i=1$, and $i=2$ denotes parameters for the virtual rotors targeting overall dynamics, interarea mode, and local mode, respectively.

In addition to the crossed cancellation of filtered signals via feedback loops, the decoupling network also consists of one bandpass filter for each target frequency. The band-pass filters are mathematically described in terms of transfer functions as

$$G_{bp}^1(s)=\frac{2\xi_1\omega_1 s}{s^2+2\xi_1\omega_1 s+\omega_1^2} \tag{7}$$

$$G_{bp}^2(s)=\frac{2\xi_2\omega_2 s}{s^2+2\xi_2\omega_2 s+\omega_2^2} \tag{8}$$

where $\omega_1$ and $\omega_2$ are target frequencies, and $\xi_1$ and $\xi_2$ are the filter damping ratios.

To facilitate the performance analyses and parameter tuning, Fig. 6 can be equivalently represented as in Fig. 8 in which the coupling interactions are presented as transfer functions. That is, the decoupling network is equivalently represented by the following transfer functions.

$$G_{f1}(s)=\frac{G_{bp1}-G_{bp1}G_{bp2}}{1-G_{bp1}G_{bp2}} \tag{9}$$

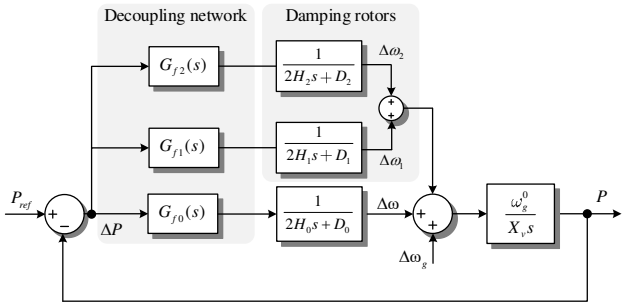


**Fig. 8. Equivalent block diagram of the MRVM. Detailed block diagram of the proposed MRVM.**

$$G_{f2}(s)=\frac{G_{bp2}-G_{bp1}G_{bp2}}{1-G_{bp1}G_{bp2}} \tag{10}$$

$$G_{f0}(s)=1-G_{f1}-G_{f2} \tag{11}$$

Note that the Laplace operator $s$ is omitted on the right-hand side of (9), (10), (11) for the sake of simplicity.

From (5), (6), and Fig. 8, the closed-loop transfer function of the MRVM can be derived as

$$G_{P2P}^{MRVM}(s)=\frac{G_{ma}(G_{f0}G_{sw0}+G_{f1}G_{sw1}+G_{f2}G_{sw2})}{1+G_{ma}(G_{f0}G_{sw0}+G_{f1}G_{sw1}+G_{f2}G_{sw2})} \tag{12}$$

$$G_{\omega 2P}^{MRVM}(s)=\frac{G_{ma}}{1+G_{ma}(G_{f0}G_{sw0}+G_{f1}G_{sw1}+G_{f2}G_{sw2})} \tag{13}$$

According to the control diagram depicted in Fig. 8, the control parameters can be tuned to maximize the damping of the MRVM. In order to simplify the tuning procedure, it is convenient to set the damping ratio of the bandpass filters at a standard value of $1/\sqrt{2}$. Unlike the bandpass filters which are only used to implement the decoupling network, the emulated swing equations can dictate the damping of the MRVM. As there are multiple swing equations in the MRVM, it would be simpler to tuning their parameters one by one. Though not strictly required, virtual motors for most unstable modes can be tuned first in order to achieve the required stability requirement. After that, one might proceed with the tuning of other virtual rotors.

For demonstrating the tuning procedure, the parameters of the VMRM are given as in TABLE I. Note that the final values of $\zeta_1$ and $\zeta_2$ are obtained after the tuning process. Though all the parameters are tunable, only two of them are essential for defining the damping of the MRVM. These two parameters are the damping ratios of the additional swing equations. From Fig. 8 and TABLE I, the frequency responses of the MRVM from grid frequency $\omega_g$ to output power $P$ can be obtained as in Fig. 9 and Fig. 10. The former shows the gain and phase of the MRVM at 0.4 Hz (inter-area mode) and 1.25 Hz (local mode), which are the frequencies of target modes when $\zeta_1$ is varied from 0.2 to 1. It can be observed that as $\zeta_1$ increases,

This article has been accepted for publication in a future issue of this journal, but has not been fully edited. Content may change prior to final publication. Citation information: DOI 10.1109/ACCESS.2021.3112070, IEEE Access



TABLE I
PARAMETERS OF THE MRVM

| Symbol | Quantity | Values: Tuning $\zeta_1$ | Values: Tuning $\zeta_2$ | Values: Final value |
|---|---|---|---|---|
| $\omega_1$ | Centre frequency of band-pass filter (rad/s) | 0.4 | 0.4 | 0.4 |
| $\xi_1$ | Damping ratio of band-pass filter | 0.707 | 0.707 | 0.707 |
| $\omega_2$ | Centre frequency of band-pass filter (rad/s) | 1.25 | 1.25 | 1.25 |
| $\xi_2$ | Damping ratio of band-pass filter | 0.707 | 0.707 | 0.707 |
| $H_0$ | Inertia constant (s) | 5 | 5 | 5 |
| $\zeta_0$ | Damping ratio | 0.707 | 0.707 | 0.707 |
| $H_1$ | Inertia constant (s) | 5 | 5 | 5 |
| $\zeta_1$ | Damping ratio | [0.3, 1] | 0.707 | 0.8 |
| $H_2$ | Inertia constant (s) | 5 | 5 | 5 |
| $\zeta_2$ | Damping ratio | 0.707 | [0.2, 1] | 0.31 |
| $\omega_g^0$ | Grid nominal frequency (Hz) | 60 | 60 | 60 |
| $X_v$ | Virtual impedance (pu) | 0.3 | 0.3 | 0.3 |

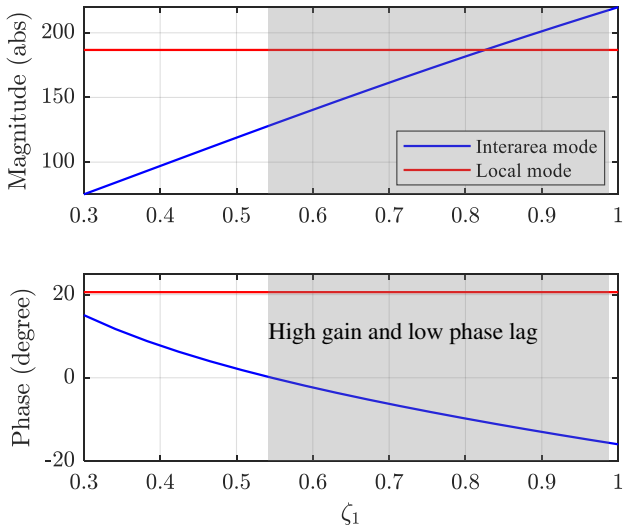


**Fig. 9. Phase and gain at 0.4 Hz (blue) and 1.25 Hz (red) for different values of $\zeta_1$**

only the gain and phase at 0.4 Hz is affected, meaning that $\zeta_1$ affects only the response of the VMRM to oscillations at 0.4 Hz. This property is achieved thanks to the decoupling network. Additionally, it is clearly shown that $\zeta_1$ is proportional to closed-loop gain and inversely proportional to phase delay. In fact, as the damping increases, the closed-loop gain of the MRVM also increases while its phase delay decreases. According to [33], the damping to LFO is maximized when the phase difference is close to zero and the gain is high. Such a condition is roughly indicated by the shadowed region in Fig. 9. In this region, the gain is significantly high while the phase displacement is relatively low. The values of the damping ratio $\zeta_1$ in this region can be

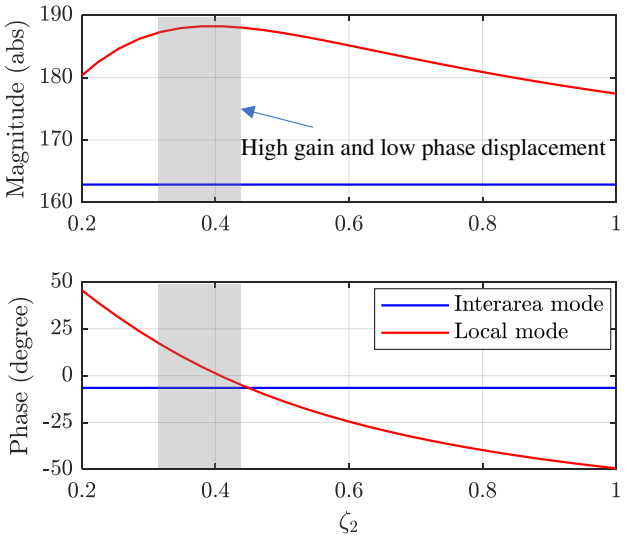


**Fig. 10. Phase and gain at 0.4 Hz (blue) and 1.25 Hz (red) for different values of $\zeta_2$**

considered for generic settings of the MRVM when the details of the grid model are unavailable.

Once, the proper damping for interarea mode is specified, a similar procedure can be carried out to determine the $\zeta_2$. Fig. 10 shows the frequency response of VRVM at 0.4 Hz and 1.25 Hz for different values of $\zeta_2$. Owing to the decoupling network, $\zeta_2$ modifies only the gain and phase of VRMR at 1.25 Hz. From such frequency characteristics, one can easily identify the feasible region for $\zeta_2$. The highlighted area showed in Fig. 10 indicates the range of value for $\zeta_2$ where the phase displacement is minimal and gain is maximized. In this case, as the variation in gain is insignificant, the overall damping is mainly determined by the phase displacement. This tuning procedure is not only useful to determine tentative parameters from the MRVM but also is important for understanding the working principles of the controller.

The proposed parameter tuning procedure can be summarized as follows:

*Input parameters*: $H_0$, $\zeta_0$, $X_v$, $\omega_g^0$, $\omega_1$, and $\omega_2$

*Tuning parameters*: $H_1$, $H_2$, $\zeta_1$ or $D_1$, $\zeta_2$ or $D_2$, $\xi_1$, and $\xi_2$

*Step* 1: set $\xi_1 = \xi_2 = 1/\sqrt{2}$ to have well-damped filters.

*Step* 2: set $H_1 = H_2 = H_0$ for simplification.

*Step* 3: set $\zeta_2 = \zeta_0$ and use (13) to find a high damping range for $\zeta_1$.

*Step 4:* Select a value for $\zeta_1$, then use (13) to high damping range for $\zeta_2$.

*Step 5*: If the simulation model of the target power system is available, *step* 3 and *step* 4 can be repeated with the modal analysis approach to fine-tune the values of $\zeta_1$ and $\zeta_2$, which will be illustrated in section IV.

This article has been accepted for publication in a future issue of this journal, but has not been fully edited. Content may change prior to final publication. Citation information: DOI 10.1109/ACCESS.2021.3112070, IEEE Access



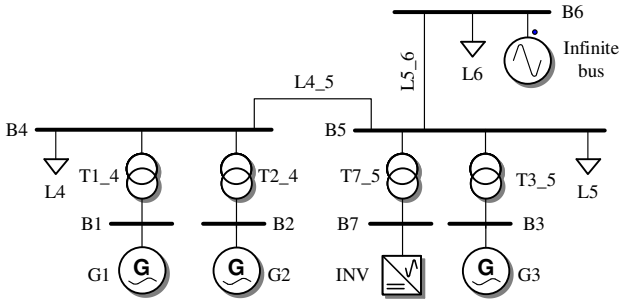


**Fig. 11. Modified three-machine-infinite-bus system.**

It is to remark that there are in fact only two tuning parameters, $\zeta_1$ and $\zeta_2$, after the simplification made in *step* 1 and *step* 2.

## IV. VALIDATION

To validate the proposed MRVM, the three-machine-infinite-bus (3MIB) system is adopted. 3MIB is an IEEE benchmark system that is commonly used to assess PSS performance when multiple modes are considered [36]. As its name suggests, the 3MIB system consists of three generators (G1, G2, and G3) and an infinite bus. Due to low damping, G1 and G2 oscillate against G3, forming local or intra-area oscillations at 1.25 Hz. At the same time, the three generators oscillate against the infinite bus at 0.4 Hz representing an interarea mode. As a modification to the original 3MIB to take into account the integration of renewables in power systems, a grid-connected power converter of 200 MW is connected to B5 through a step-up transformer. The complete model for validating the proposed control scheme is depicted in Fig. 11. The parameters of the MRVM are given in TABLE I and are the same for all simulations. The following modal analysis and time-domain results are obtained by using PowerFactory software. The eigenvalue loci are achieved by combining the simulation results from hundreds of simulations for all the values of the damping ratios.

Fig. 12 shows the local and interarea modes for two cases: (i) base case in which the power converter is controlled as a grid-following power converter (GFLC), and (ii) when the conventional SPC-GFMC is employed. It is clear from this figure that the system is unstable due to the fact that the real part of the interarea mode is positive. As soon as the SPC is employed, the interarea mode moves further to the left-hand-side plane with around 8% damping. This increase indicates that the SPC provides significant damping to the interarea mode. On the other hand, the local mode is almost not affected by the conventional SPC-GFMC. This is consistent with the analysis carried out in the previous section that the SPC is able to provide damping to oscillatory modes whose frequency is lower than 1 Hz. In fact, the SPC can only increase the damping of local mode to just above 3% which is unsatisfactory according to grid codes where at least 5% damping is required [37].

For tuning the parameters of the MRVM, the feasible regions in the previous section can be used when the details of the grid model are unavailable. In contrast, when the grid

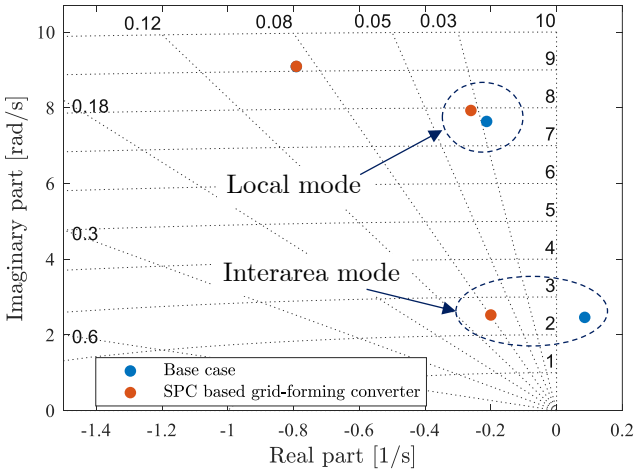


**Fig. 12. Low-frequency modes of the modified 3MIB system.**

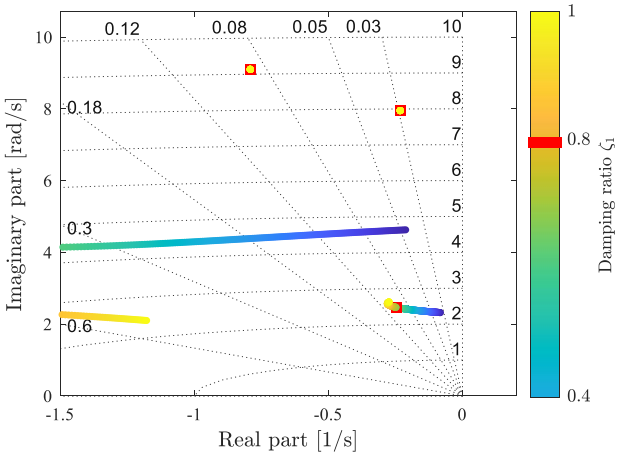


**Fig. 13. Eigenvalue locus of the 3MIB system when MRVM is employed and $\zeta_1$ is varied.**

model is known, the settings of damping ratios for the MRVM can be further specified using eigenvalue locus. Specifically, Fig. 13 shows the mode trajectories when the damping ratio $\zeta_1$ is varied from 0.4 to 1. It can be seen that by increasing $\zeta_1$, the damping of interarea mode is increased from around 3% to approximately 11%. As the $\zeta_1$ approach 0.9, the system damping starts to decreases due to the increase in phase displacement discussed in the previous section. Thus, the damping ratio can be conservatively chosen as $\zeta_1 = 0.8$. Comparing to the SPC-GFMC, the damping of interarea mode is increased from 8% to 11%. This result reveals that MRVM does not only improve system stability but also it allows specifying the desired damping. Interestingly, the local mode is almost unaffected by $\zeta_1$.

Considering $\zeta_1 = 0.8$, Fig. 14 shows the eigenvalue locus of the 3MIB system for different values of $\zeta_2$. It can be seen that $\zeta_2$ can significantly improve the damping of the local mode. Indeed, as $\zeta_2$ decreases, the damping of local mode is

This article has been accepted for publication in a future issue of this journal, but has not been fully edited. Content may change prior to final publication. Citation information: DOI 10.1109/ACCESS.2021.3112070, IEEE Access



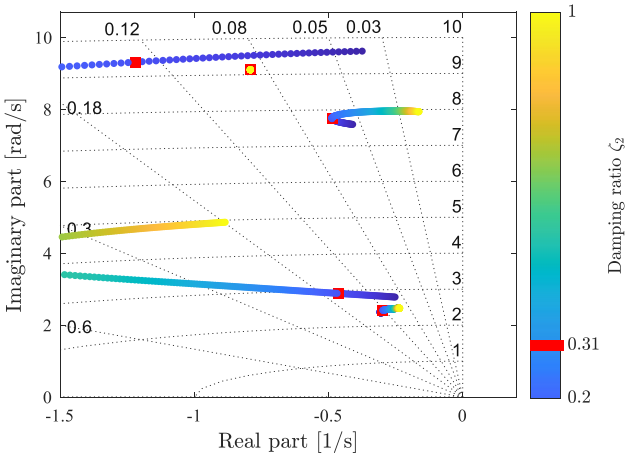


**Fig. 14. Eigenvalue locus of the 3MIB system when MRVM is employed and $\zeta_2$ is varied.**

increased from 2% to around 6.5% at $\zeta_2 = 0.31$. Such improvement of the damping ratio clearly confirms that MRVM is more effective than the SPC which can only bring this damping ratio to just above 3%. Moreover, slight coupling between the damping ratio $\zeta_2$ and the interarea mode can be observed. This coupling is, however, beneficial because it brings the interarea mode further to the left-hand side of the complex plane, increasing the damping ratio of the interarea mode to 12%.

Fig. 13 and Fig. 14 clearly confirm that (i) the feasible regions defined with the single converter infinite bus system in Fig. 6 encompass the optimal settings of the MRVM for an actual grid; (ii) the tuning of the control parameters is nearly decoupled meaning that the virtual rotors can be separately tuned; (iii) MRVM is more effective than conventional GFMC in damping LFO.

To further illustrate the performance of the MRVM, comparative simulations of the modified 3MIB system have been conducted. Fig. 15 shows the time domain simulation results of the 3MIB system for different control schemes of the grid-connected converter. The considered test cases are: (i) GFLM, (ii) SPC-GFMC, (iii) MRVM with a virtual rotor tuned for interarea mode, and (iv) MRVM with two virtual rotors tuned for interarea mode and local mode. To generate an event, a reactive load is connected at B5 at $t$ = 1 s and then disconnected at $t$ = 1.1 s.

Fig. 15 (a) and Fig. 15 (b) shows the active power delivered by the generator G1, G2, and G3, and Fig. 15 (c) shows the power injected by the power converter. As can be clearly seen in the base case, the system experiences sustained oscillations with increasing amplitude, which is due to the unstable pole associated with the interarea interactions. On the other hand, the SPC-GFMC is able to attenuate the interarea oscillations moving the system into a more stable state. Nevertheless, as the SPC-GFMC is unable to improve the damping of the local mode, the local oscillation is sustained for an extended period. Such oscillations can be observed more clearly in the output power of G1 and G2. A slight improvement to damping of

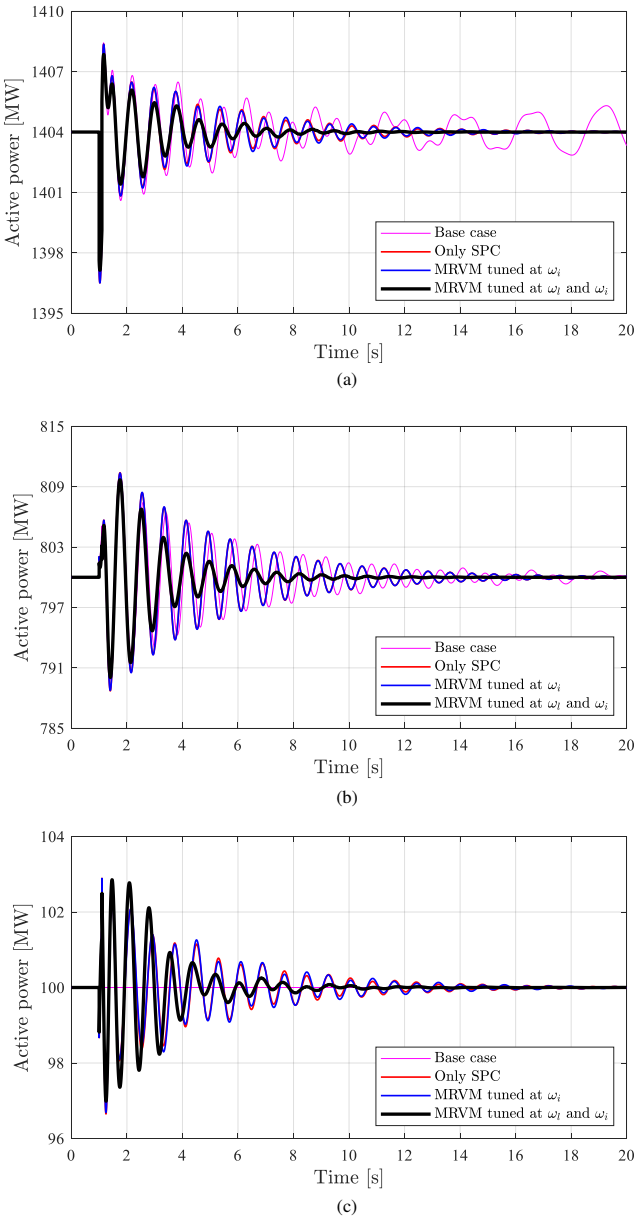


**Fig. 15. Active power injected by the generators and the GFMC for different control strategies; (a) Active power of G1 and G2; (b) Active power of G3; (c) Active power of the converter.**

interarea mode can be observed when the MRVM is tuned for $\omega_1$.

When MRVM tuned at $\omega_1$ and $\omega_2$ is employed, both local and interarea interactions are improved. In fact, power oscillations completely vanish after 8 seconds instead of 15 seconds as in the case of the SPC-GFMC. Fig. 15 (c) also indicates that MRVM reduces the oscillations of the injected power by the power converter. Consequently, these results further confirm that the MRVM can provide superior performance over conventional GFMC in terms of attenuating power oscillations.

In addition to the higher damping at critical modes provided, Fig. 16 reveals that the MRVM also improves the

This article has been accepted for publication in a future issue of this journal, but has not been fully edited. Content may change prior to final publication. Citation information: DOI 10.1109/ACCESS.2021.3112070, IEEE Access



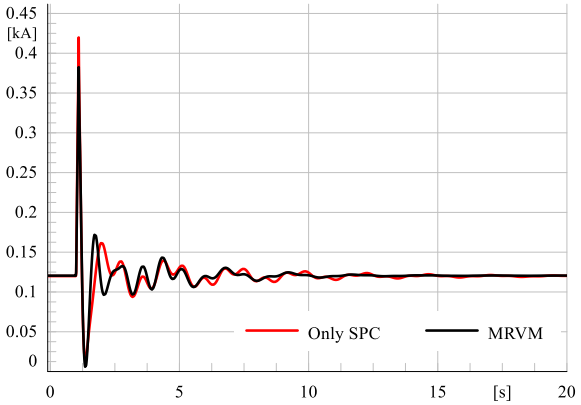


**Fig. 16. Current injected by the GFMC with different controllers.**

transient performance of the GFMC. That is the peak current at the moment of the event is lower when MRVM is employed. Moreover, the power oscillations at the output of the GFMC also decay faster. It is evident that the MRVM enhance the transient response of both the grid and the converter.

## VII. CONCLUSION

This paper proposes a multi-rotor virtual machine (MRVM) controller for improving the attenuation to SSR in power systems. As a proof of concept, the MRVM is proposed assuming the inner control loop of the power converter is well designed and able to handle adverse operating conditions of the grid such as voltage sag or distortion. The MRVM leverages the flexibility offered by the digital implementation of GFMC's control system to emulate a VSM with multiple rotors. Each of the virtual rotors can be tuned separately to achieve desired performance such as overall electromechanical response or LFO damping. Additionally, a decoupling network for enhancing signal filtering is employed to eliminate the coupling between the virtual rotors, which not only improves the overall performance but also facilitates the tuning of the control parameters. In addition to formalizing the concept, this paper also proposes tuning strategies for the MRVM by using frequency-domain and modal analyses. Simulation results of MRVM with the IEEE 3MIB system confirms that the MRVM is an effective and flexible solution in dealing with power resonances. Future work would focus on the validation of the proposed MRVM in experimental settings.

## REFERENCES

[1] G. Rogers, *Power System Oscillations*. Boston, MA: Springer US, 2000.

[2] J. Paserba, J. Sanchez-Gasca, L. Wang, P. Kundur, E. Larsen, and C. Concordia, "Small-Signal Stability and Power System Oscillations," 2012, pp. 1–24.

[3] K. Prasertwong, N. Mithulananthan, and D. Thakur, "Understanding Low-Frequency Oscillation in Power Systems," *Int. J. Electr. Eng. Educ.*, vol. 47, no. 3, pp. 248–262, Jul. 2010.

[4] N. Hatziargyriou *et al.*, "Stability definitions and characterization of dynamic behavior in systems with high penetration of power electronic interfaced technologies," 2020.

[5] I. Dobson *et al.*, "Electric Power Transfer Capability: Concepts, Applications, Sensitivity, Uncertainty," New York, 2001.

[6] F. Demello and C. Concordia, "Concepts of Synchronous Machine Stability as Affected by Excitation Control," *IEEE Trans. Power Appar. Syst.*, vol. PAS-88, no. 4, pp. 316–329, Apr. 1969.

[7] F. Schleif, H. Hunkins, G. Martin, and E. Hattan, "Excitation Control to Improve Powerline Stability," *IEEE Trans. Power Appar. Syst.*, vol. PAS-87, no. 6, pp. 1426–1434, Jun. 1968.

[8] D. N. Walker, C. E. J. Bowler, R. L. Jackson, and D. A. Hodges, "Results of subsynchronous resonance test at Mohave," *IEEE Trans. Power Appar. Syst.*, vol. 94, no. 5, pp. 1878–1889, Sep. 1975.

[9] X. Xie, X. Guo, and Y. Han, "Mitigation of Multimodal SSR Using SEDC in the Shangdu Series-Compensated Power System," *IEEE Trans. Power Syst.*, vol. 26, no. 1, pp. 384–391, Feb. 2011.

[10] J. Adams, C. Carter, and S.-H. Huang, "ERCOT experience with Sub-synchronous Control Interaction and proposed remediation," in *PES T&D 2012*, 2012, pp. 1–5.

[11] Z. Assi Obaid, L. M. Cipcigan, and M. T. Muhssin, "Power system oscillations and control: Classifications and PSSs' design methods: A review," *Renew. Sustain. Energy Rev.*, vol. 79, pp. 839–849, Nov. 2017.

[12] PES, "IEEE Recommended Practice for Excitation System Models for Power System Stability Studies," *IEEE Std 421.5-2005 (Revision IEEE Std 421.5-1992)*, vol. 2005, no. April, pp. 0_1-85, 2006.

[13] F. Rashidi and M. Rashidi, "Robust and Adaptive Tuning of Power System Stabilizers Using Artificial Neural Networks," in *Innovations in Applied Artificial Intelligence*, 2004, pp. 1023–1032.

[14] J. Fang, H. Li, Y. Tang, and F. Blaabjerg, "On the Inertia of Future More-Electronics Power Systems," *IEEE J. Emerg. Sel. Top. Power Electron.*, vol. 7, no. 4, pp. 2130–2146, 2019.

[15] G. Cao, Z. Y. Dong, Y. Wang, P. Zhang, and Y. T. Oh, "VSC based STATCOM controller for damping multi-mode oscillations," in *2008 IEEE Power and Energy Society General Meeting - Conversion and Delivery of Electrical Energy in the 21st Century*, 2008, pp. 1–8.

[16] K. M. Son and J. K. Park, "On the robust LQG control of TCSC for damping power system oscillations," *IEEE Trans. Power Syst.*, vol. 15, no. 4, pp. 1306–1312, 2000.

[17] G. S. Chawda, A. G. Shaik, O. P. Mahela, S. Padmanaban, and J. B. Holm-Nielsen, "Comprehensive Review of Distributed FACTS Control Algorithms for Power Quality Enhancement in Utility Grid With Renewable Energy Penetration," *IEEE Access*, vol. 8, pp. 107614–107634, 2020.

[18] F. H. Gandoman *et al.*, "Review of FACTS technologies and applications for power quality in smart grids with renewable energy systems," *Renew. Sustain. Energy Rev.*, vol. 82, pp. 502–514, Feb. 2018.

[19] X. Sui, Y. Tang, H. He, and J. Wen, "Energy-Storage-Based Low-Frequency Oscillation Damping Control Using Particle Swarm Optimization and Heuristic Dynamic Programming," *IEEE Trans. Power Syst.*, vol. 29, no. 5, pp. 2539–2548, Sep. 2014.

[20] M. Li, L. Xiong, H. Chai, L. Xiu, and J. Hao, "Mechanism of PV Generation System Damping Electromechanical Oscillations," *IEEE Access*, vol. 8, pp. 135853–135865, 2020.

[21] N. B. Lai, S. Member, K. Kim, and P. Rodriguez, "Voltage Sensorless Control Scheme based on Extended-State Estimator for a Grid-Connected Inverter," *IEEE Trans. Power Electron.*, vol. PP, no. c, p. 1, 2019.

[22] N. B. Lai, A. Tarraso, G. N. Baltas, L. Marin, and P. Rodriguez, "Inertia Emulation in Power Converters with Communication Delays," in *2020 IEEE Energy Conversion Congress and Exposition (ECCE)*, 2020, pp. 1665–1669.

[23] R. Rosso, X. Wang, M. Liserre, X. Lu, and S. Engelken, "Grid-Forming Converters: Control Approaches, Grid-Synchronization, and Future Trends—A Review," *IEEE Open J. Ind. Appl.*, vol. 2, pp. 93–109, 2021.

[24] A. Tayyebi, F. Dörfler, F. Kupzog, Z. Miletic, and W. Hribernik, "Grid-Forming Converters – Inevitability, Control Strategies and

Challenges in Future Grids Application," *CIRED Work. 2018*, no. 0236, pp. 1–5, 2018.

[25] P. Christensen *et al.*, "High Penetration of Power Electronic Interfaced Power Sources and the Potential Contribution of Grid Forming Converters," 2020.

[26] W. Zhang, "Control of grid connected power converters with grid support functionalities," Universitat Politècnica de Catalunya, 2017. [Online]. Available: https://upcommons.upc.edu/bitstream/handle/2117/110897/TWZ1de1.pdf'

[27] M. Abdollahi, J. I. Candela, J. Rocabert, M. A. Elsaharty, and P. Rodriguez, "Novel Analytical Method for Dynamic Design of Renewable SSG SPC Unit to Mitigate Low-Frequency Electromechanical Oscillations," *IEEE Trans. Power Electron.*, vol. 35, no. 7, pp. 7532–7544, Jul. 2020.

[28] G. N. Baltas, N. B. Lai, L. Marin, A. Tarraso, and P. Rodriguez, "Grid-Forming Power Converters Tuned Through Artificial Intelligence to Damp Subsynchronous Interactions in Electrical Grids," *IEEE Access*, vol. 8, pp. 93369–93379, 2020.

[29] G. N. Baltas, N. B. Lai, A. Tarraso, L. Marin, F. Blaabjerg, and P. Rodriguez, "AI-Based Damping of Electromechanical Oscillations by Using Grid-Connected Converter," *Front. Energy Res.*, vol. 9, Mar. 2021.

[30] "IEEE Standard for Interconnecting Distributed Resources with Electric Power Systems," *IEEE Std 1547-2003*, pp. 1–28, 2003.

[31] E. O. Netz, "REQUIREMENTS FOR OFFSHORE GRID CONNECTIONS IN THE E.ON NETZ NETWORK," 2008.

[32] P. Rodriguez, C. Citro, J. I. Candela, J. Rocabert, and A. Luna, "Flexible Grid Connection and Islanding of SPC-Based PV Power Converters," *IEEE Trans. Ind. Appl.*, vol. 54, no. 3, pp. 2690–2702, 2018.

[33] N. J. Kundur, P. and Balu, *Power System Stability and Control*. McGraw-Hill, 1994.

[34] M. Beza and M. Bongiorno, "An Adaptive Power Oscillation Damping Controller by STATCOM With Energy Storage," *IEEE Trans. Power Syst.*, vol. 30, no. 1, pp. 484–493, Jan. 2015.

[35] M. Klein, G. J. Rogers, and P. Kundur, "A fundamental study of inter-area oscillations in power systems," *IEEE Trans. Power Syst.*, vol. 6, no. 3, pp. 914–921, 1991.

[36] C. Canizares *et al.*, "Benchmark Models for the Analysis and Control of Small-Signal Oscillatory Dynamics in Power Systems," *IEEE Trans. Power Syst.*, vol. 32, no. 1, pp. 715–722, Jan. 2017.

[37] S. Mendoza-Armenta and I. Dobson, "Applying a Formula for Generator Redispatch to Damp Interarea Oscillations Using Synchrophasors," *IEEE Trans. Power Syst.*, vol. 31, no. 4, pp. 3119–3128, Jul. 2016.

**NGOC BAO LAI** (Student Member, IEEE) received the B.S. degree in electrical engineering from Danang University of Science and Technology, Da Nang, Vietnam, in 2014, and the M.S. degree in electrical and information engineering at Seoul National University of Science and Technology, Seoul, Korea, in 2017. He is currently pursuing a Ph.D. degree in electric energy systems at Universitat Politècnica de Catalunya (UPC), Spain and at Luxembourg Institute of Science and Technology (LIST), Luxembourg. His research interests include power electronics, power system stability, and networked control of distributed generation systems.

**GREGORY N. BALTAS** (Student Member, IEEE) received the B.S. degree in electrical engineering from the Technological Educational Institute of Central Greece, Chalkis, Greece, in 2015, and the M.S. degree in power engineering from the University of Sydney, Sydney, Australia. He is currently pursuing the Ph.D. degree in data science with the Universidad Loyola Andalucía. Since 2018, he has been a Research Assistant with the Loyola Institute of Science and Technology (Loyola.TECH), Universidad Loyola Andalucía. His research interests include applied artificial intelligence, power system stability, and autonomous energy systems.

**PEDRO RODRIGUEZ** (F'13) received his M.Sc. and Ph.D. degrees in electrical engineering from the Technical University of Catalonia (UPC), Spain (1994 and 2004, respectively). He was a postdoc researcher at the CPES, Virginia Tech, US, at the Department of Energy Technology, Aalborg University (AAU), Denmark and at the MIT Energy Initiative (MITie), Boston, US. He was a co-supervisor of the Vestas Power Program, Denmark (2007 – 2011). He was a director of technology on Modern Power Systems at Abengoa Research (2011-2017). From 2017, he is a full professor at the Loyola University Andalucia, where he is the Head of LOYOLA.Tech, leading a research programme on Intelligent Energy Systems. He is also linked with the UPC as a parttime professor. He is in the Clarivate's list of Highly Cited Researchers in Engineering (2015-2018). He has co-authored one Wiley-IEEE book, more than 100 papers in ISI technical journals, and around 300 papers in conference proceedings. He is the holder of 16 licensed patents. He has participated in more than 50 projects with industrial partners and several EU projects. Dr. Rodriguez is an IEEE Fellow for his contributions in the control of distributed generation. He has served as an Associate Editor of the IEEE Transaction on Power Electronics, IEEE Journal on Emerging and Selected Topics on Power Electronics, IEEE Journal on Industrial Electronics and Energies. His research interests include intelligent energy systems, distributed generation, and universal energy access.